doi:10.3969/j.issn.1673-9736.2018.02.04
Article ID: 1673-9736(2018)02-0114-06

3D fast inversion of gravity data based on GPU

WANG Xusheng and ZENG Zhaofa

College of Geo-Exploration Science and Technology, Changchun 130026, China

Abstract: Large-scale gravity 3D interpretation depends on efficient and high-resolution 3D inversion processing of massive data. The authors applied the conjugate gradient method with minimum support function and prior model constraint to reduce multi-solutions in gravity inversion. Based on the parallel programming and computing platform NVIDIA CUDA with C++ language, we achieve fast 3D gravity inversion by adopting GPU parallel technique into the most time consuming part relating to sensitivity matrix. The results of theoretical model show that the abnormal body can be clearly located and the inversion speed is improved greatly. Comparing with inversion speed of the Matlab program, speed of inversion with GPU parallel technique has improved more than 100 times under the hardware condition of Geforce GTX 1060 graphics card.

Key words: GPU; CUDA; gravity inversion; conjugate gradient method

0 Introduction

Gravity exploration, with the advantages of lightweight, fast speed, less investment, is widely used in oil and gas exploration, mineral exploration and the study of deep earth structure and other fields (Nabighian M N *et al.*, 2005). With the rapid development of computer and the increasing requirements of gravity exploration, the 3D inversion of gravity data has become a research hot, however, the 3D inversion still has two problems, one is the multi-solution problem, another is the calculation efficiency. In geophysical inversion, the generation of multiple solutions is due to the error of measured data, the discrete and sparse data, and the equivalence of field sources. Generally, increasing the field observation data and improving the observation accuracy can reduce the multiple solvability of the inversion. Regarding to the multiple solutions caused by the equivalence of field sources, we can solve the problem by adding constraints and prior information in inversion. Last & Kubik (1983) first considered the minimum gradient support function in compact gravity inversion. Guillen & Menichetti (1984) used the similar principle into gravity and magnetic inversion by minimizing the moment of inertia. Portniaguine & Zhdaov (1999) discussed the focusing inversion and showed that they could more precisely locate geophysical anomalies using this algorithm. Silva *et al.* (2001) discussed a variety if constraint methods. Zhdanov (2009) discussed the focusing inversion and its improvement in detail. Li & Oldenburg (1998) applied a "smooth inversion" method to gravity data inversion. Geng *et al.* (2014) applied variogram to the inversion of gravity gradient data. Liu *et al.* (1997) use genetic algorithm to 2D density interface inversion. CHEN Hua-gen *et al.* (2002) applied improved simulated annealing method into gravity inversion. Geng *et al.* (2013) used neu-

Received 5 December 2017, accepted 14 January 2018
Supported by Project of Geophysical Comprehensive Survey and Information Extraction of Deep Mineral Resources (No. 2016YFC0600505).

ral network method into 2D gravity inversion. Chen *et al.* (2013) applied pre-conjugate gradient method to the inversion of gravity gradient data. Feng *et al.* (2014) constrained the basin model by the total variation function, and retrieved the basin basement by gravity data. Chen *et al.* (2014) applied focusing inversion into inversion of gravity gradient. Liu Yan *et al.* (2015) conducted 3D gravity inversion using Bayesian method based on model reduction. Geng *et al.* (2016) applied cokriging method into gravity gradient data inversion.

3D Gravity inversion divides the observed subsurface media into small non-overlapping units, and then calculate the density of each discrete element by the inversion method to determine the actual distribution of field sources. With the expansion of measurement area and the improvement of precision, the mesh quantity of subdivision is massive, and the inversion calculation takes a lot of time. Yao *et al.* (2003) optimized the matrix storage and improved the inversion efficiency according to the special relationship between gridding survey points and underground subdivision. Chen *et al.* (2012) achieved the 3D fast forward modeling of gravity and gravity gradient using GPU. Hou *et al.* (2015) used GPU for fast speed inversion calculation of gravity gradient data.

In view of the above mentioned two gravity inversion technical problems, this paper applies the principle of focusing inversion to inverse gravity data using conjugate gradient method. In this paper, several key problems in the parallel computation of inversion are analyzed, and the 3D conjugate gradient gravity fast inversion based on GPU parallel technology of NIVIDIA CUDA platform is achieved, due to the good parallel improvement ability of conjugate gradient inversion. The experimental results show that the method can well determine the abnormal location, and the inversion efficiency is greatly improved.

1 Forward theory

By the law of gravity, the forces of any point in the geologic body acting in the outer space is:

$$V(\vec{r}) = G\iiint \frac{\rho}{\vec{r}}dV \tag{1}$$

where $\vec{r}$ is a vector from observation point $P(x,y,z)$ to $Q(\xi,\eta,\zeta)$ which is in the geological body, and G is gravitational constant.

In 3D inversion, underground space is divided into cuboid units of equal size and compact arrangement like Fig. 1. Analytical formulas for gravity and gravity gradient forward modeling in rectangular space is shown as below:

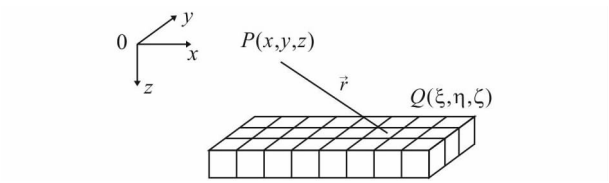

Fig. 1 Sketch map of subdivision model

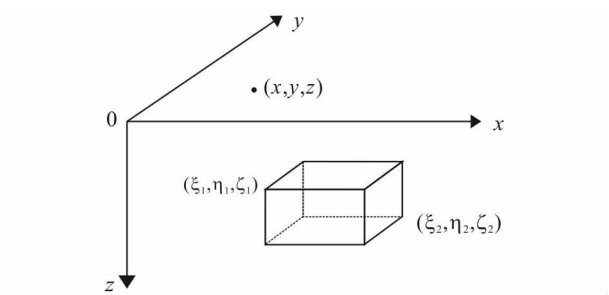

Fig. 2 Sketch map of observation points and geological body

Like the underground space coordinate system shown in Fig. 2, the x axis and y axis are in the horizontal direction, and the Z axis is vertical downward. Coordinate of observation point is (x,y,z), $(\xi,\eta,\zeta) \in [\xi_1, \xi_2] \times [\eta_1,\eta_2] \times [\zeta_1,\zeta_2]$. It's a volume element of any cuboid in space and gravity anomalies and gravity gradients produced by this element (Guo *et al.*, 2004) is

$$V_z = -G\rho\sum_{i=1}^{2}\sum_{j=1}^{2}\sum_{k=1}^{2}\mu_{ijk}x_i\left[\ln(y_j + r_{ijk}) + y_j\ln(x_i + r_{ijk}) + z_k\arctan\frac{z_k r_{ijk}}{x_i y_j}\right] \tag{2}$$

$$V_{xx} = G\rho\sum_{i=1}^{2}\sum_{j=1}^{2}\sum_{k=1}^{2}\mu_{ijk}\arctan\frac{y_j z_k}{x_i r_{ijk}} \tag{3}$$

$$V_{yy} = G\rho\sum_{i=1}^{2}\sum_{j=1}^{2}\sum_{k=1}^{2}\mu_{ijk}\arctan\frac{x_i z_k}{y_j r_{ijk}} \tag{4}$$

$$V_{zz} = G\rho \sum_{i=1}^{2}\sum_{j=1}^{2}\sum_{k=1}^{2}\mu_{ijk}\arctan\frac{x_i y_j}{z_k r_{ijk}} \quad (5)$$

$$V_{xy} = -G\rho \sum_{i=1}^{2}\sum_{j=1}^{2}\sum_{k=1}^{2}\mu_{ijk}\ln(z_k + r_{ijk}) \quad (6)$$

$$V_{xz} = -G\rho \sum_{i=1}^{2}\sum_{j=1}^{2}\sum_{k=1}^{2}\mu_{ijk}\ln(y_j + r_{ijk}) \quad (7)$$

$$V_{yz} = -G\rho \sum_{i=1}^{2}\sum_{j=1}^{2}\sum_{k=1}^{2}\mu_{ijk}\ln(x_i + r_{ijk}) \quad (8)$$

Where $x_i = x - \xi_i$, $y_i = y - \eta_j$, $z_i = z - \xi_k$, $r_{ijk} = \sqrt{x_i^2 + y_j^2 + z_k^2}$, $\mu_{ijk} = (-1)^{i+j+k}$.

Underground space is divided into cuboid units of equal size and compact arrangement, and each unit is set as a fixed residual density value. We assume underground space is divided into M cuboid elements and the observation surface is arranged with N observation points. And the gravity anomaly of j th ($j = 1, \cdots, M$) element in i th ($i = 1, \cdots, N$) observation point is

$$d_{\alpha\beta}^{i} = G_{ij}m_j \quad (9)$$

Where m_j is residual density value of jth element and G_{ij} represent the geometric framework ith cuboid. According to the principle of potential field superposition, the total anomaly at the ith observation point is the sum of the anomalies of the underground j cuboid:

$$d_{\alpha\beta} = \sum_{i=1}^{M} d_{\alpha\beta}^{i} = \sum_{i=1}^{M} G_{ij}m_j \quad (10)$$

express as matrix form

$$\begin{bmatrix} d_{\alpha\beta}^{1} \\ d_{\alpha\beta}^{2} \\ ? \\ d_{\alpha\beta}^{N} \end{bmatrix} = \begin{bmatrix} G_{11} & G_{12} & \cdots & G_{1M} \\ G_{21} & G_{22} & & \vdots \\ \vdots & & \ddots & \vdots \\ G_{N1} & \cdots & \cdots & \vdots \end{bmatrix} \cdot \begin{bmatrix} m_1 \\ m_2 \\ \vdots \\ m_M \end{bmatrix} \quad (11)$$

is same as

$$d_{\alpha\beta} = G_{\alpha\beta}m \quad (12)$$

Where $d_{\alpha\beta}$ is observed data, m is residual density, $G_{\alpha\beta}$ is response of the j th cuboid at the i th observation point which is called sensitivity matrix.

2 Inversion theory

The solution of geophysical inverse problems is often ill conditioned. Tikhonov regularization method is often used to solve the problem. The objective function can be expressed as

$$\varphi(m) = \varphi_d + \mu\varphi_m \quad (13)$$

Where μ is regularization factor, φ_d is fitting difference function which usually expressed in terms of L_2 norm like

$$\varphi_d = \| d - Gm \|_2^2 \quad (14)$$

In the weighted focus inversion algorithm, the minimum support function is introduced as

$$S_{MS}(m) = \sum_{j=1}^{M} \frac{m_j^2}{m_j^2 + \beta^2} \quad (15)$$

Where β is smaller constants to avoid generating singular values when m_j equal to zero. At the same time, in order to avoid the skin effect, we add the sensitivity matrix based on weighted function

$$w_j = \left(\sum_{i=1}^{N} G_{ij}\right)^{\beta/4}, j = 1, \ldots, M \quad (16)$$

so

$$\varphi(m) = \| Gm - d \|^2 + \mu \sum_{j=1}^{M} \frac{w_j m_j^2}{m_j^2 + \beta^2} \quad (17)$$

There is an existence of a diagonal matrix

$$W(m) = diag\left[\left(\frac{m^2 + \beta^2 I}{w_j}\right)^{1/2}\right] \quad (18)$$

The upper form can be rewritten as

$$\varphi(m) = \| GWW^{-1}m - d \|^2 + \mu \| w^{-1}m \|^2 \quad (19)$$

Assuming $m_w = w^{-1}m$, $G_w = GW$, then

$$\varphi(m) = \| G_w m_w - d \|^2 + \mu \| m_w \|^2 \quad (20)$$

The inversion problem is taken into account

$$\begin{bmatrix} GW \\ \sqrt{u}I \end{bmatrix} m_w = \begin{bmatrix} d \\ 0 \end{bmatrix} \quad (21)$$

Substituting $A = \begin{bmatrix} GW \\ \sqrt{u}I \end{bmatrix}$, $b = \begin{bmatrix} d \\ 0 \end{bmatrix}$, into formula 21, the formula 21 can be written in the following form:

$$Am_w = b \quad (22)$$

We use the conjugate gradient method for solving the above equation, and pseudo code is as follows:

Input: G, d, μ, k

Output: m

Begin

set $m_0 = 0$

compute W, m_{w0}, G_{w0}

set $A = \begin{bmatrix} GW \\ \sqrt{u}I \end{bmatrix}$, $b = \begin{bmatrix} d \\ 0 \end{bmatrix}$

$k = 0$; $g = 2A^{\mathrm{T}}(Am_{w0} - b)$

while $g_0 \neq 0$

$k = k + 1$

if $k = 1$

$p_1 = -g_0$

else

$\beta_k = g_{k-1}^{\mathrm{T}} g_{k-1} / g_{k-2}^{\mathrm{T}} g_{k-2}$

$p_k = -g_{k-1} + \beta_k p_{k-1}$, $q_k = g_{k-1}^{\mathrm{T}} p_k$

$m_{wk} = m_{wk-1} + \alpha p_k$

Update m, W, A, g_k

End

where k is number of iterations, g_k is gradient of objective function, p_k is search direction, β_k is step length of nonlinear exact line search.

3 Inversion results

It is assumed that there are zones with maximum buried depth of 1000 m, and axial and longitudinal range from −1 000 m to 1 000 m. Underground space has two residual density 0.5 g/cm^3 cuboid anomaly with size of 300 m × 400 m × 500 m and anomaly centers located at (−450 m, 0 m, −450 m) and (450 m, 0 m, −450 m). Computational domain [−1 000 m, 1 000 m] × [−1 000 m, 1 000 m] × [−1 000 m, 0 m] is divided into 20 × 20 × 10 small units, each unit is 100 m × 100 m × 100 m. The observation point is set on the ground with $z = 0$. There are total 20 lines designed with line interval of 100 m, point interval of 100 m, and there are 20 × 20 points in total. Fig. 3 shows the plane inversion profile of inversion results of $z = 500$ m and $y = 0$ m. The abnormal body boundary position of the actual theoretical model is indicated by the black frame in the Fig 3. From the Figure, it is indicated that the weighted focus inversion has a good effect, which can reflect the location and burial depth of the abnormal body.

4 GPU parallel theory

In recent years, GPU technology has developed rapidly. CUDA (Compute Unified Devices Architecture) was Launched in 2006 by NVIDIA, the GPU of which can be used for general calculation. The programming mode is using CPU as the host, for logical and serial computing, and GPU, as a device, is for executing highly parallel thread tasks.

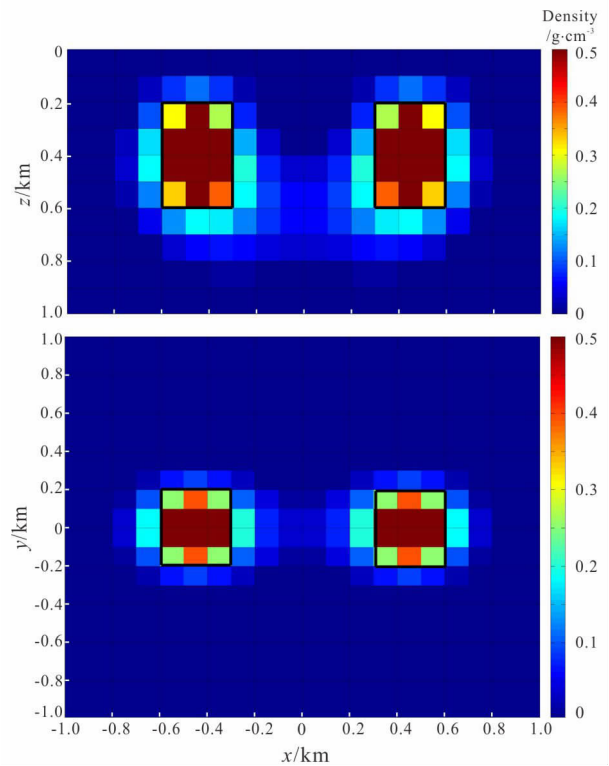

(a) Section $y = 0$; (b) section $z = 500$.

Fig. 3 Inversion results of the two abnormal bodies in underground space model

Matlab are usually used for calculation, which belong to interpretative language with low efficiency. C++ calculation that has higher computational efficiency than Matlab is used in this study. In the gravity inversion, because of the large sensitivity matrix, the corresponding calculation part of sensitivity matrix needs to consume a large amount of time. It is also the main reason for making inversion time consuming. The algorithm is shown in Fig. 4. By parallel computing g_k and G_{wk}, an obvious acceleration effect is achieved. In addition, in the parallel computation, due to repeated call for sensitivity matrix iteration, even if the GPU interface transmission bandwidth is large, it also needs to consume a lot of time. By sto-

ring the sensitivity matrix in the GPU memory, the whole inversion process only need to be passed from the host once therefore it accelerates the speed of inversion without multiple transmissions.

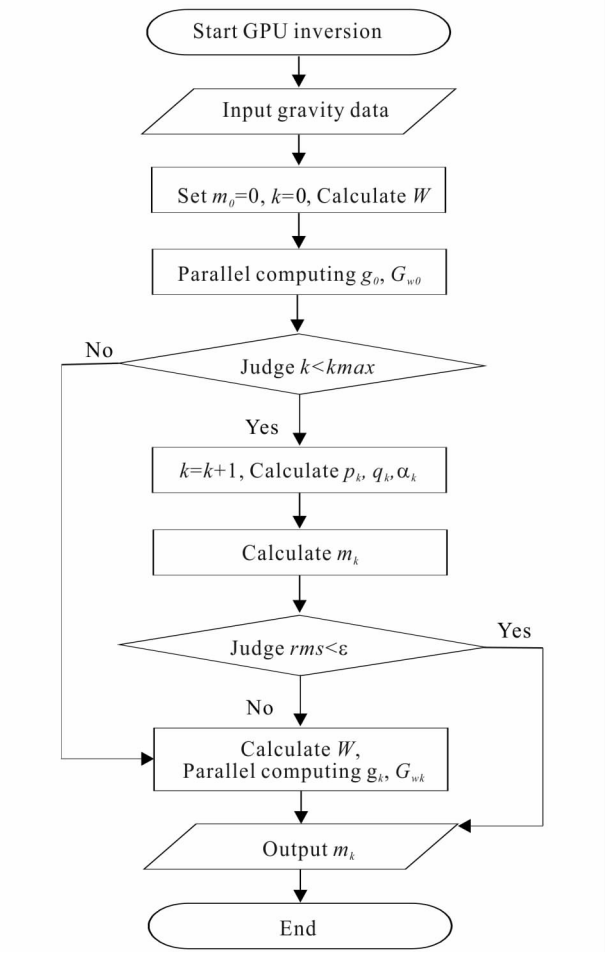

Fig. 4 Flow of GPU parallel computing algorith

Table 1 Comparison of time consuming among GPU and Matlab

Model size	GPU consuming/s	Matlab consuming/s
10 × 10 × 10	1.85	16.10
20 × 20 × 10	16.41	297.83
30 × 30 × 10	32.70	1717.30
40 × 40 × 10	64.66	5002.43
50 × 50 × 10	103.48	12369.36

5 GPU parallel result analysis

The numerical test hardware environment used in this paper: i7 6700k CPU, 4 GHz main frequency and 8G memory. GPU model is Geforce GTX 1060 with 1280 processing cores, 6G memory and computing capacity of 6.1. Software environment is CUDA 8.0 version, Windows10 64 bits operating system and Visual Studio 2015 compiler. The calculating time spent in iterating 100 times is compared between Matlab and GPU parallel in scales of 1 000 m × 1 000 m × 1 000 m, 2 000 m × 2 000 m × 1 000 m, 3 000 m × 3 000 m × 1 000 m, 4 000 m × 4 000 m × 1 000 m and 5 000 m × 5 000 m × 1 000 m, and grid partition is dx = 100 m, dy = 100 m, dz = 100 m. Because the GPU memory limit, we did not calculate the size of larger scale. If possible, we can use multiple GPU cards to calculate larger scale. It can be seen from Table 1 that when the scale is small, GPU parallel acceleration effect relative to the Matlab is not obvious, with the acceleration effect only ten times better, but with the increase of the size of the GPU model, calculation efficiency is obviously improved, finally accelerating effect can be more than 100 times better than Matlab.

6 Conclusion

In this study, we firstly established a model with two separated abnormal bodies, then we got the inverson result from the gravity data. It is indicated that the gravity focusing inversion has a good effect to reflect the gravity abnormal. After that, we researched rapid inversion of gravity data and achieved fast gravity inversion based on conjugate gradient method using GPU parallel technique. The result showed that the algorithm has a high speedup ratio. The GPU parallel technique and its realization in gravity inversion provide technical support for fast 3D large-scale gravity inversion. It can also provide references for inversion methods like simulated annealing, genetic algorithm and artificial neural network algorithm.

Acknowledgements

We are particularly grateful to Professor Huang Danian. Specially thanks to the project teams of Geophysical Comprehensive Survey, and to all the experts who have put efforts into this paper.

References

Chen H G, Wu J S, Wang J L. 2002. Research in modified simulated annealing gravity inversion. *Journal of Jilin University* (*Earth Science Edition*), **32**(3):294-298. (in Chinese with English abstract)

Chen S H, Zhu Z Q, Lu G Y, *et al*. 2013. Inversion of gravity gradient tensor based on preconditioned conjugate gradient. *Journal of Central South University*: *Science and Technology*, **44**(2):619-625. (in Chinese with English abstract)

Chen Y, Li T L, Fan C S, *et al*. 2014. The 3D focusing inversion of full tensor gravity gradient data based on conjugate gradient. *Progress in Geophysics*, **29**(3):1133-1142. (in Chinese with English abstract)

Chen Z X, Meng X H, Guo L H, *et al*. 2012. 3D fast forward modeling and the inversion strategy for large scale gravity and gravimetry data based on GPU. *Chinese Journal of Geophysics*, **55**(12):4069-4077. (in Chinese with English abstract)

Feng X L, Wang W Y, Liu F Q, *et al*. 2014. 2D gravity inversion of basement relief of rift basin based on a dual interface model. *Chinese Journal of Geophysics*, **57**(6): 1934-1945. (in Chinese with English abstract)

Geng M X, Huang D N, Yang Q, *et al*. 2014. 3D inversion of airborne gravity-gradiometry data using cokriging. *Geophysics*, **79**(4):G37-G47.

Geng M X, Huang D N, Yu P, *et al*. 2016. 3D constrained inversion of full tensor gradiometer data based on cokriging method. *Chinese Journal of Geophysics*, **59**(5): 1849-1860. (in Chinese with English abstract)

Geng M X, Yang Q J. 2013. 2D density inversion with the RBF neural network method. *Oil Geophysical Prospecting*, **48**(4):651-657. (in Chinese with English abstract)

Guillen A, Menichetti V. 1984. Gravity and magnetic inversion with minimization of a specific functional. *Geophysics*, **49**(8):1354-1360.

Guo Z H, Guan Z N, Xiong S Q. 2004. Cuboid ΔT andits gradient forward theoretical expressions without analytic odd points. *Chinese Journal of Geophysics*, **47**(6): 1131-1138. (in Chinese with English abstract)

Hou Z L, Wei X H, Huang D N, *et al*. 2015. Full tensor gravity gradiometry data inversion: Performance analysis of parallel computing algorithms. *Applied Geophysics*, **12**(3):292-302.

Last B J, Kubik K. 1983. Compact gravity inversion. *Geophysics*, **48**(6):713-721.

Li Y, Oldenburg D W. 1998. 3-D inversion of gravity data. *Geophysics*, **63**(1):109-119.

Liu Y F, Shen X H. 1997. Nonlinear inversion of gravity anomalies caused by 2D surface of geologic structures genetic algorithms. *Computing Techniques for Geophysical and Geochemical Exploration*, **19**(2):138-142. (in Chinese with English abstract)

Liu Y, Lv Q T, Li X B, *et al*. 2015. 3D gravity inversion based on Bayesian method with model order reduction. *Chinese Journal of Geophysics*, **58**(12):4727-4739. (in Chinese with English abstract)

Nabighian M N, Ander M E, Grauch V J S, *et al*. 2005. Historical development of the gravity method in exploration. *Geophysics*, **70**(6): 63-89.

Portniaguine O, Zhdanov M S. 1999. Focusing geophysical inversion images. *Geophysics*, **64**(3):874-887.

Silva J B C, Medeiros W E, Barbosa V C F. 2001. Potential-field inversion: Choosing the appropriate technique to solve a geologic problem. *Geophysics*, **66**(2):511-520.

Yao C L, Hao T Y, Guan Z N, *et al*. 2003. High-speed computation and efficient storage in 3D gravity and magnetic inversion based on genetic algorithms. *Chinese Journal of Geophysics*, **46**(2): 252-258. (in Chinese with English abstract)

Zhdanov M S. 2009. New advances in regularized inversion of gravity and electromagnetic data. *Geophysical Prospecting*, **57**(4):463-478.